(NASA-TM-79158) MEASUREMENTS OF MIXED CONVECTIVE HEAT TRANSFER TO LOW TEMPERATURE HELIUM IN A HORIZONTAL CHANNEL (NASA) 16 p HC A02/MF A01 CSCL 20D G3/34

N79-23384

Unclas 22087

DOE/NASA/0207-79/3
NASA TM-79158

MEASUREMENTS OF MIXED CONVECTIVE HEAT TRANSFER TO LOW TEMPERATURE HELIUM IN A HORIZONTAL CHANNEL

V. M. Yeroshenko, Ye. V. Kuznetsov, O. A. Shevchenko
Ministry of Power and Electrification
Krzhizhanovsky Power Engineering Institute

Robert C. Hendricks
National Aeronautics and Space Administration
Lewis Research Center

D. E. Daney
National Bureau of Standards
Institute for Basic Standards

Work performed for
U. S. DEPARTMENT OF ENERGY
Office of Energy Technology
Division of Electric Energy Systems

TECHNICAL PAPER
Fifteenth International Congress on Refrigeration
sponsored by the International Institute of Refrigeration
Venice, Italy, September 23-29, 1979

DOE/NASA/0207-79/3
NASA TM-79158

MEASUREMENTS OF MIXED CONVECTIVE HEAT TRANSFER TO LOW TEMPERATURE HELIUM IN A HORIZONTAL CHANNEL

V. M. Yeroshenko, Ye. V. Kuznetsov, O. A. Shevchenko
Ministry of Power and Electrification
Krzhizhanovsky Power Engineering Institute
Moscow, U.S.S.R.

Robert C. Hendricks
National Aeronautics and Space Administration
Lewis Research Center
Cleveland, Ohio U.S.A. 44135

D. E. Daney
National Bureau of Standards
Institute for Basic Standards
Boulder, Colorado U.S.A. 80302

Prepared for
U.S. DEPARTMENT OF ENERGY
Office of Energy Technology
Division of Electric Energy Systems
Washington, D.C. 20545
Under U.S. - U.S.S.R. Energy Agreement Subtask 080207

Fifteenth International Congress on Refrigeration
sponsored by the International Institute of Refrigeration
Venice, Italy, September 23-29, 1979

MEASUREMENTS OF MIXED CONVECTIVE HEAT TRANSFER TO LOW TEMPERATURE HELIUM IN A HORIZONTAL CHANNEL

V.M. Yeroshenko, Ye.V. Kuznetsov, O.A. Shevchenko
The Krzhizhanovsky Power Engineering Institute - Moscow, U.S.S.R.
Robert C. Hendricks
NASA-Lewis Research Center - Cleveland, Ohio 44135 USA
D.E. Daney
Institute for Basic Standards, NBS - Boulder, Colorado 80302 USA

E-014

1. INTRODUCTION

Attempts to use widely superconducting large scale systems give an impetus to comprehensive investigations on methods of cryogenic stabilization. Comparing the alternative procedures, it becomes clear, particularly for superconducting power transmission lines, that the advantageous approach consists in cooling superconductors by forced circulation of supercritical helium /1/. There are several papers /2-7/ presenting experimental data on forced convection heat transfer to supercritical helium. It is worth while noting that these papers have successfully correlated their experimental data with an accuracy of about ±30%, but have failed to correlate the data presented in different papers. This is an evidence of either insufficient measurement accuracy or inadequate knowledge of the physical processes under study. Most experiments have been carried out with ducts of relatively small diameters (1-2 mm). As a consequence, the effect of geometry and body forces on heat transfer was negligible and, therefore, unaccounted for in the correlations. Ref. /8/ reported on the heat transfer to supercritical helium in vertical ducts of a comparatively large diameter (18 mm); but for proposed designs of superconducting power transmission lines /9/, generally rather large (>> 1÷2 mm) horizontal coolant flow channels are envisioned. In the near-critical region, thermophysical properties are very sensitive to heat input; thus one would expect substantial secondary flow effects in a heated long horizontal channel of sufficiently large diameter (much greater than 1÷2 mm). This assumption follows from the similarity theory; indeed, the considerable nonuniformity of wall temperature distribution over the periphery of a horizontal tube cooled by the flow of supercritical water or CO_2 has been verified experimentally and studied in depth /10-21/. But a dearth of experimental data on combined free and forced convective heat transfer to supercritical helium exists in literature. It is obvious that such information is of importance for superconducting power transmission line design when fault conditions are under consideration and in all cases when heat input to the superconductor becomes more than its steady state value - e.g., due to leakage in vacuum space or short circuiting. The data may be also useful for designers of any large helium cooling systems.

Along with the experimental approach there are attempts to obtain data on heat transfer to supercritical helium using the similarity theory in conjunction with generalized empirical relationships for other supercritical media /22/. The attempts appear to be rather successful /23/ but reliable results for an unstudied range of parameters with large thermogravitational effects could not be insured.

In this paper we have extended our preliminary results /24/ on the measurements of combined free and forced convective heat transfer to supercritical helium flow and attempt to explain and correlate the data.

The experimental conditions covered correspond to usually recommended parameters for SPTL projects /9/.

2. APPARATUS & ANALYSIS

The experimental set-up is that described in /24/ and is in part repeated here only as a convenience to the reader.

In the flow loop schematic, Fig. 1, helium flows from the refrigerator-liquifier 1 to the test channel 5 via a cryogenic pipeline 2 and distribution head 3 of control unit 4. For closed loop operation, the helium flow from channel 5 is delivered through a return pipe to refrigerator 1 cooling the radiation shields of channel 5, unit 4 and pipeline 2. For open loop operation, the helium flows from channel 5 to a gasholder via an open valve of unit 4, heat exchanger 6 and flowrate measuring section 7. In both cases the main parameters of the flow (p, T, G) were determined by the refrigerator-liquifier setting and controlled by means of throttle valves of head 3 and unit 4.

Liquid nitrogen cooled shields were used to reduce heat input to the helium flow loop from room temperature.

Fig. 2 shows the stainless steel horizontal circular test channel. A manganin wire heater is wound with a 4 mm pitch on the 2.85 m long, 2.0 cm o.d., 1.9 cm i.d. heated section of channel 5. A stainless steel, 6 mm o.d., 5 mm i.d. rotatable co-axial probe enables one to obtain temperature profiles at two cross-sections of the flow. When the probe is rotated, its thermocouples describe circles of 4, 5.5, 7, 8.5 mm radii.

The inlet $\overline{T_{b1}}$, and outlet $\overline{T_{b2}}$ bulk fluid temperatures were measured with arsenide-gallium resistance thermometers introduced into the flow downstream of mixing chambers at either end of the test section where velocity and temperature profiles over the cross-section are averaged. Temperature profiles along the test section wall, over its periphery and at two flow cross-sections were measured by copper-iron thermocouples /25/. Positions of the thermocouples and thermometers are shown in Fig. 3.

Without heating, $\overline{T_{b1}}$, and $\overline{T_{b2}}$ agreed to within 0, 02 K. Errors in temperature measured with differential thermocouples were less than 0.2 K. The variation of bulk fluid temperature $\overline{T_b}$ along the test section was calculated from inlet temperature, pressure and heat input (the pressure drop along the heated section was negligible). For open cycle operation the mass flowrate obtained from the heat-balance was compared with the more accurate orifice flowmeter (at room temperature); the comparison served as one validity criteria for the experimental procedure.

For closed loop operation, the flowrate was determined only from the heat-balance equation but preliminary calibration with the orifice flowmeter was carried out for every run. Values of mass flowrate determined by these two methods agreed to within ±5%.

Helium properties needed in the analysis were determined from /26/, stainless steel conductivity data /27/ were used to calculate the inner wall temperature of the heated section by means of an iteration procedure.

Experimental results

A more detailed analysis of the data than appears in /24/ is presented as Table I; also listed are computed parameters required in the analysis that follows.

The use of the equivalent-hydraulic diameter D_H as a characteristic size agrees well (±3%) with the correlation

$$\frac{Nu}{Nu_\infty} = 1 - \frac{0.45}{2.4 + Pr}\left(\frac{d}{D}\right)^{0,6}$$

proposed /29/ for annular tubes with heat input only to outer tube, for the range of parameters covered in these experiments (d/D = 0.3).

Wall temperature distribution over the heated section periphery

The temperature distribution (Fig. 4) at $x/L = 0.57$ was measured by eight thermocouples equally spaced on the tube periphery. The profiles are typical of flows in heated horizontal tubes, that is, the highest temperatures are observed in the upper surface while the lowest ones occur on the lower surface. We compared profiles obtained ($60 < Gr_q/Gr_L < 600$; $x/L = 0.57$) with those calculated from correlation /31/

$$\frac{T_w - T_{w_\pi}}{T_{w_0} - T_{w_\pi}} = \cos^n\left(\frac{\phi}{2}\right) \qquad (1)$$

where for the steady flow with near-ideal properties at $Re = 8.5 \cdot 10^3$ to $5.2 \cdot 10^4$, $Gr_q = (0.2 \text{ to } 2) \cdot 10^9$, $T_w/\bar{T}_b = 1.05$ to 1.3 where $Gr_q/Gr_L < 250$, $n = f(Gr_q/Gr_L)$ and $n = 2$ at $Gr_q/Gr_L > 250$ to 300 (solid curves in Fig. 4). It can be seen that experimental and calculated values agree qualitatively. But it should be noted that in all regimes (test runs) the measured temperature exceeds the calculated one at $\phi = \pi/4$ and in regimes 2, 6 and 10, the first temperature being even higher than that on the upper surface. It is unlikely that this could be attributed to experimental errors since each point was covered by two thermocouples. Further wall temperature ripples can be assumed to be associated with features of flow structure in horizontal tubes and caused by the effect of secondary flows.

Temperature distribution in helium flow

Fig. 5 gives the typical temperature distribution obtained for regime 2 at $x/L = 0,4$. Isotherms are plotted on the basis of local flow temperature profiles measured by the probe. The pattern of isotherms is typical of flows with mixed convection. It is of interest to note that the maximum difference between local temperatures in the upper and lower parts of the flow were measured to be 6.1 K while the maximum difference between measured wall temperature was about 3.0 K. This significant discrepancy can be attributed to the presence of low temperature zones in the flow. The isotherm pattern found evidence also of the existence of a cell-wise flow structure brought about by secondary flows of thermogravitational origin. Examining the changes in the pattern of isotherms, it can be concluded that the flow includes six vortices.

In the upper part of the channel the gradient dT/dh on all lines with $h =$ const is directed towards the vertical axis. Thus, the isotherms indicate that there exists an upward flow along the vertical axis. At the angle of $\phi \approx \pi/3$ the isotherms undergo changes; curves begin to bend downwards approaching the wall. Evidently, the flow heated up from the wall in the middle portion of the channel and moving along the wall downwards and, as a result of their interaction, the first flow begins to move towards the channel axis. Also, there is a zone with the rapid rise in temperature gradient, $dT/d\phi$ at $\phi \approx 0.8\,\pi$ which indicates the existence of secondary flow. Judging by isotherm shapes, it may be assumed that the flow in the zone is directed from the channel axis to its wall. Due to a relatively great distance between thermocouple junctions (about 1.5 mm) and to low temperature gradients at $\phi \approx \pi$, it proved to be impossible to obtain the complete picture of secondary flows at the bottom of the channel. However, the character of flows in adjacent regions of the channel suggests that an upward flow takes place at $\phi \approx \pi$ along the vertical axis. Therefore the temperature distribution in the flow implies that there are at least six large vortices in the channel, which are in contrast to the isothermal surfaces, constant property photographs in /24/.

The flow pattern obtained allows some features of temperature distribution over the wall periphery to be explained. Evidently, the highest wall temperature is unlikely to be found in the upper surface exposed to secondary flows coming from cooler fluid layers but near the region with $\phi = \pi/3$ where two secondary flows with the highest energies merge.

This is responsible for a relative rise in wall temperature at $\phi = \pi/4$. At the same time, it might be expected that the wall temperature at the lowest surface exceed those at $\phi = 0.8\,\pi$. But this appeared to be true only in regime 2 while in regime 15 the opposite effect was observed and in all other regimes the feature was not noted at all. Thus, it can be assumed that in the lower portion the flow structure is more complex than that shown in Fig. 5 and depends on regime parameters; perhaps the behavior is more closely related to developing forced convection flow.

Wall temperature distribution along the heated section

Fig. 6 shows wall temperature profiles along the upper and lower surfaces of the channel. Calculated values of bulk fluid temperature $\bar{T}_b$ are also plotted. The maximum temperature difference over the wall periphery is seen to be equal to 8.7 K (regime 10) which should be considered as a rather significant value if it is taken into account that bulk fluid temperature was 12.5 K. Also the data presented show that entrance and exit portions of the duct have some influence on the wall temperature profiles. Comparing changes in wall and flow temperatures it may be assumed that the lengths of the flow thermal stabilization are different for upper and lower wall surface that is, the length for upper surface appears to be 1.5 times less than that for the lower one.

Heat transfer coefficients

Assuming (1) adequately describes the peripherial surface temperature, and taking $n = 2$

$$\overline{\alpha}_\phi = \frac{q_w}{\sqrt{\left(T_{w_0} - \overline{T}_b\right)\left(T_{w_\pi} - \overline{T}_b\right)}} = \sqrt{\alpha_{\phi=0} \cdot \alpha_{\phi=\pi}}$$

where $\overline{\alpha}_\phi = \frac{1}{\pi}\int_0^\pi \alpha(\phi)d\phi$; and since $Nu_\phi = \frac{\alpha_\phi D_H}{\lambda_b}$, it follows that* $\overline{Nu}_\phi =$

$\sqrt{Nu_{\phi=0} \cdot Nu_{\phi=\pi}}$ for three tube cross-sections ($x/L = 0.375$; 0.57; 0.759) where thermal stabilization of the flow has been achieved.

An attempt was made to generalize the data by the relationship /23/ proposed for supercritical turbulent forced flows at large Reynolds numbers

$$Nu_r = \frac{Nu}{Nu_b} = \begin{cases} \psi^{-0.55} \equiv f_1 & (2a) \\ \text{or} & \\ \left(\frac{2}{\sqrt{0.8\,\psi + 0.2} + 1}\right)^2 \equiv f_2 & (2b) \end{cases}$$

where for our results the local parameter ψ_ϕ replaces ψ and f_1 or f_2 group the data with the same rapport, $f_1 \sim f_2 \rightarrow f$. As for the lower surface, our data agree with Eq. (2) satisfactorily enough; 73% of points deviate from the predicted curve (Fig. 7(a)) only by ±20%.

Therefore, we believe the heat transfer on the lower wall surface within the range of parameters covered to be weakly dependent on the thermogravitational effect and, thus, can be estimated by usual correlations (Eq. (2)).

The application of a single parameter ψ to correlate experimental data obtained for the upper wall surface proved to be inadequate; all experimental points fall below the predicted curve by 50% on the average. As a consequence, the correlation of Nu_ϕ values by Eq. (2) was also unsuccessful, and experimental data were by 20 ÷ 30% below the predicted curve, see also /24/. This is quite conceivable since Eq. (2) does not include a term accounting for the effects of secondary flows due to thermogravitation on heat transfer.

To correlate experimental data on the upper surface we modified the relationship /31/

$$\frac{Nu_{\phi=0}}{Nu_T} = \frac{1 + 0.035\left(\frac{Gr_q}{Gr_L}\right)^{0.43}}{\left[1 + \left(\frac{Gr_q}{Gr_L}\right)^3\right]^{0.048}} \equiv f_3$$

where Nu_T is the turbulent Nusselt number to:

$$Nu_{r_{\phi_0}} = \frac{Nu_{\phi=0}}{Nu_b} = f \cdot f_3 \qquad (3)$$

*Form similar to van der Waals binary mixture rule and differs from that of /24/ where $\overline{Nu}_\phi = xNu_0 + (1 - x)Nu_\pi$ and $\overline{\psi} = x\psi_0 + (1 - x)\psi_\pi$ with $x =$ $\frac{1}{\pi}\int_0^\pi \left(\frac{T - T_\pi}{T_0 - T_\pi}\right)d\phi$ and $D_H = D - d$.

This data representation as compared to (2) turned out to be more attractive, since nearly all points were within the range of ±30%. Heat transfer deterioration at $\phi = 0$ due to free convection influence causes the general reduction of $\overline{Nu}_\phi$ in comparison with purely forced flow. The deterioration of $\overline{Nu}_\phi$ seems to be related to the trend to suppress the turbulent flow in the upper portion of the channel. It is evident that the suppression exceeds additional flow turbulence near the lower surface. Using correlations (2) and (3) in conjunction with (1), the expression to estimate average heat transfer for combined free and forced convection for a horizontal channel can be derived

$$\overline{Nu}_{r_\phi} = \frac{\overline{Nu}_\phi}{Nu_b} = f\sqrt{f_3} \qquad (4)$$

where $\psi = \psi_\phi = 1 + \beta(\overline{T}_{W\phi} - \overline{T}_b)$, $\overline{T}_{W\phi}$ - the wall temperature averaged over its periphery, Eq. (4) has been substantiated by our experiments and predicts experimental data with an accuracy of about ±20% (Fig. 7).

3. CONCLUSIONS

An experimental study on heat transfer to low temperature helium flow in a horizontal channel where thermogravitational forces affect the flow considerably has been carried out.

It has been found that there are six vortices causing an upward flow in the upper portion of the channel which gives rise to a shift in the location of the highest temperature from the uppermost point on the wall surface to the point at $\phi \approx \pi/3$.

Wall temperature profiles have been obtained. The contradiction between the measured temperature distribution over the tube wall periphery and that given by Eq. (1)) can be attributed to the effect of secondary flows caused by thermogravitational forces.

The thermal stabilization length on the lower wall is demonstrated to be on the average 1.5 times greater than that on the upper surface.

Experimental data on local heat transfer both on the lower and upper wall surfaces have been correlated using the parameter Gr_q/Gr_L, accounting for the effect of thermogravitational forces, and the local parameter $\psi_\phi = 1 + \beta(T_{W\phi} - \overline{T}_b)$. It is found that the heat transfer coefficient for the lower surface has the same value as in the case of flow without free convection effects.

To estimate the heat transfer coefficient averaged over the wall periphery, it is proposed to use for horizontal tubes the dependence $\overline{Nu}_{r\phi} = f(\overline{\psi}_\phi)$ where $\overline{\alpha}_\phi = \sqrt{\alpha_{\phi 0} \cdot \alpha_{\phi\pi}}$.

4. NOMENCLATURE

x	axial distance from heated section inlet	Q	heater electric power
		$\pi DL = F_p$	heated surface area
L	length of the heated section	$\beta = -\frac{\partial \ln \rho}{\partial T}$	isobaric expansion coefficient
D	(heated section); inner diameter	g	gravitational acceleration
d	(probe); outer diameter	ρ	density
$\sqrt{D^2 - d^2} = D_H$	equivalent hydraulic diameter	ϕ	angle; $\phi = 0$ uppermost tube surface; $\phi = \pi$ lowest tube surface
T	temperature	$\frac{4}{\pi}\frac{G}{\mu D_H} = Re$	Reynolds number
μ	viscosity		
λ	heat conductivity	$\frac{\mu C_p}{\lambda} = Pr$	Prandtl number
G	mass flow rate		
C_p	specific heat	$\frac{g q_w \rho^2 \beta D_H^4}{\lambda \mu^2} = Gr_q$	Grashof number
p	pressure		

$\frac{q_w D_H}{(T_{w_\phi} - \overline{T}_b)\lambda} = Nu_\phi$	local Nusselt number	$\frac{Gr_q}{Gr_L}$	thermogravitational forces parameter (see /13/, /30/, /31/)
		h	distance from the horizontal surface
$1 + \beta(T_w - \overline{T}_b) = \psi$	non-isothermal parameter /23/	$q_w = \frac{Q}{F_p}$	
$1 + \beta(T_{w_\phi} - \overline{T}_b) = \psi_\phi$	local non-isothermal parameter	Subscripts:	
$0.023\ Re^{0.8} Pr^{0.4} = Nu_b$	Dittus-Boelter dependence	ϕ	local
		C	upper surface
α	heat transfer coefficient	π	lower surface
		w	wall
$\frac{Nu}{Nu_b} = Nu_r$	reduced Nusselt number	b	bulk
Gr_L	limit value of the Grashof number;	—	value averaged over the wall periphery

$$Gr_L = 3\cdot 10^{-5}\cdot Re^{2.75}\left[1+2.4Re^{-0.125}\ (Pr^{2/3}-1)\right] Pr^{0.5}$$

5. REFERENCES

1. (a) V. ARP. "Forced Flow, Single-Phase Helium Cooling Systems", Advances in Cryogenic Engineering, Vol. 17, K. D. Timmerhaus, (ed.) Plenum Press, New York (1972), Paper J-4, pp. 342-351.
   (b) P. J. GIARRATANO, R. C. HESS and M. C. JONES, "Forced Convection Heat Transfer to Subcritical Helium I", Advances in Cryogenic Engineering, vol. 19, K. D. Timmerhaus (ed.) Plenum Press, New York (1974), Paper K-1, pp. 404-416.
2. H. H. HOLM, M. J. LEUPOLD and R. D. HAY, "Heat Transfer by the Circulation of Supercritical Helium". Advances in Cryogenic Engineering, vol. 11. K. D. Timmerhaus (ed.), Plenum Press, New York (1966), Paper H-4, pp. 530-535.
3. P. J. GIARRANTANO, V. D. ARP and R. V. SMITH, "Forced Convection Heat Transfer to Supercritical Helium". Cryogenics, vol. 11 (1971), pp. 385-393.
4. H. OGATO, and S. SATO, "Measurements of Forced Convection Heat Transfer to Supercritical Helium", Proc. Fourth International Cryogenic Engineering Conference. IPC Science and Technology Press, Ltd., Guilford, England (1972), pp. 291-294.
5. C. JOHANNES, "Studies of Forced Convection Heat Transfer to Helium-I", Advances in Cryogenic Engineering, vol. 17, K. D. Timmerhaus (ed.), Plenum Press, New York (1972), pp. 352-360.
6. P. J. GIARRANTANO, and M. C. JONES, "Deterioration of Heat Transfer to Supercritical Helium at 2.5 Atmospheres", International Journal of Heat and Mass Transfer, vol. 18 (1975), pp. 649-665.
7. V. G. PRONKO, G. P. MALYSHEV, and L. N. MIGALINSKAYA, "'Normal' and 'Deteriorated' Heat Transfer Conditions in a Single-Phase Near-Critical State During Turbulent Flow of Helium in Tubes", Fizicheskii Zhurnal, Vol. 30 (1976), pp. 606-612.
8. D. J. BRASSINGTON, and D. N. H. CAIRNS, "Measurements of Forced Convective Heat Transfer to Supercritical Helium", International Journal of Heat and Mass Transfer, Vol. 20 (1977), pp. 207-214.
9. S. FONER, and B. B. SCHWARTZ, (eds.) Superconducting Machines and Devices, Plenum Press, New York (1974).

*10. A. V. ZHUKOVSKY, Proceedings of TsKTI, 611o, Leningrad, 1970, p. 40.

*11. A. V. ZHUKOVSKY, Energomashinostroenie, N 2 (1971) 23.

12. Yu. V. VIKHROV, A. S. KONKOV, V. M. SOLOMONOV, and I. T. SINITSYN, "Heat Transfer in Horizontal and Inclined Steam-Generating Tubes at Supercritical Pressures", High Temperature, Vol. 11 (1973), pp. 1183-1185; translated from Teplofisika Visokikh Temperatur, Vol. 11 (1973), pp. 1316-1318.

*Russian text; availability in U.S. unknown.

13. B. S. PETUKHOV, A. F. POLYAKOV, and Yu. L. SHEKHTER, "Turbulent Flow and Heat Transfer in a Gravitational Field", High Temperature, Vol. 16 (1978), pp. 531-547; translated from Teplofizika Vysokikh Temperatur, Vol. 16 (1978), pp. 624-639.
14. B. S. PETUKHOV, V. S. GRIGOR'YEV, A. F. POLYAKOV, and S. V. ROSNOVSKIY, "An Experimental Study of Heat Transfer in Pipes with Variable Density of the Heat Flux Through the Wall", Heat Transfer - Soviet Research, Vol. 9 (1977), pp. 114-122.
15. B. S. PETUKHOV, and A. F. POLYAKOV, "Effect of Free Convection on Heat Transfer During Forced Flow in a Horizontal Pipe", High Temperature, Vol. 5 (1967), pp. 348-351; translated from Teplofiska Visokikh Temperatur, Vol. 5 (1967), pp. 384-387.
16. B. Ya. KAMENETSKII, "Special Features of Heat Transfer with Mixed Convection in Horizontal Tubes", Thermal Engineering, Vol. 21 (1974), pp. 84-87; translated from Teploenergetika, Vol. 21 (1974), pp. 61-63.
17. M. E. SHITSMAN, "The Effect of Natural Convection on Temperature Conditions in Horizontal Tubes at Supercritical Pressures", Thermal Engineering, Vol. 13 (1966), pp. 69-75; translated from Teploenergetika, Vol. 13 (1966), pp. 51-56.
18. Yu. D. BARULIN, Yu. V. VIKHREV, V. B. DYADYAKIN, A. N. KOBLYAKOV, A. S. KONKOV, V. A. LOKSHIN, and I. T. SINITSYN, "Heat Transfer During Turbulent Flow in Vertical and Horizontal Tubes Containing Water With Supercritical State Parameters", Journal of Engineering Physics, Vol. 20 (1971), p. 665; translated from Inzhenerno Fisicheskii Zhurnal, Vol. 20 (1971), p. 929.
19. W. B. HALL, J. D. JACKSON, and A. WATSON, "A Review of Forced Convection Heat Transfer to Fluids at Supercritical Pressures", Institution of Mechanical Engineers Symposium on Heat Transfer and Fluid Dynamics of Near Critical Fluids (1968), Paper 3.
20. N. M. SHNURR, "Heat Transfer to Carbon Dioxide in the Immediate Vicinity of the Critical Point", Journal of Heat Transfer, Vol. 91 (1969), pp. 16-20.
21. G. A. ADEBIYI, and W. B. HALL, "Experimental Investigation of Heat Transfer to Supercritical Pressure Carbon Dioxide in a Horizontal Pipe", International Journal of Heat and Mass Transfer, Vol. 19 (1976), pp. 715-720.
22. N. M. SHNURR, "Numerical Predictions of Heat Transfer to Supercritical Helium in Turbulent Flow Through Circular Tubes", Journal of Heat Transfer, Vol. 99 (1977), pp. 580-585.
23. R. C. HENDRICKS, V. M. YEROSHENKO, L. A. YASKIN, and A. D. STAROSTIN, "Bulk Expansion Factors and Density Fluctuations in Heat and Mass Transfer", to be presented at the Fifteenth International Congress of Refrigeration, Venice 23-29 (Sept. 1979), Paper B 1/119.
24. R. C. HENDRICKS, D. E. DANEY, V. M. YEROSHENKO, Ye. V. KUZNETSOV, and O. A. SHEVCHENKO, "Some Heat Transfer and Hydrodynamic Problems Associated with Superconducting Cables", DOE/NASA/0207-78/1, NASA TM-79023.
25. V. M. BEILIN, I. Ya. LEVIN, L. A. MEDVEDEVA M. P. ORLOVA, and I. L. ROGEL'BERG, "Thermocouple for Low Temperatures, Which Has an Electrode Made of Copper + Iron Alloy", Instruments and Experimental Techniques, Vol. 15 (1972), pp. 1869-1870; translated from Pribory i Tekhnika Experimenta, Vol. 15 (1972), pp. 215-216.
26. R. D. McCARTY, "Thermophysical Properties of Helium-4 from 2 to 1500 K with Pressures to 1000 Atmospheres", National Bureau Standards, NBS-TN-631 (1972).
*27. M. P. MALKOV, Handbook on physical and technical backgrounds of cryogenics, Moscow, Energiya, 1973.
*28. L. A. YASKIN, Manuscript 3207-78DEP deposited in VINITI of October 12, 1978.
*29. B. S. PETUKHOV, et al., Heat Transfer in Nuclear Power Plants, Moscow, Atomizdat, 1974, p. 254.
30. B. S. PETUKHOV, A. F. PILIAKOV, Yu. L. SHEKHTER, and V. A. KULESHOV, "Experimental Study of the Effect of Thermal Gravitation Upon Turbulent Flow and Heat Transfer in Horizontal Pipes", Heat Transfer and Turbulent Buoyant Convection, Vol. 2, D. B. Spalding and N. Afgan (eds.), Hemisphere Publishing Corp., Washington, D.C. (1977), pp. 719-727.
31. B. S. PETUKHOV, A. F. POLYAKOV, V. A. KULESHOV, and Yu. L. SHEKHTER, "Turbulent Flow and Heat Transfer in Horizontal Tubes with Substantial Influence of Thermogravitational Forces", Heat Transfer-1974, Vol. III, Japan Society of Mechanical Engineers, Tokyo (1974), pp. 164-168.

ACKNOWLEDGEMENT: The assistance of J. R. Hendricks in preparing this document is greatly appreciated.

*Russian text; availability in U.S. unknown.

L'ETUDE EXPERIMENTALE DE LA TRANSMISSION DE CHALEUR PAR CONVECTION AU HELIUM AUPRES DE CRITIQUE DANS LE CANAL HORIZONTAL

SOMMAIRE: On mesure les coefficients de la transmission du chaleur au hélium auprès de critique, coulant dans un tube chaufe de longueur horizontale 2.85 m et de diamètre intérieur 19 mm. La gamme des paramètres expérimentaux comprend 6.5 - 15 K; 1.2 - 3.0 bar aux flux de chaleur jusqu'à 1000 W/m^2 et les nombres de Reynolds sont de l'ordre de 9.10^3 à 2.10^5. On trouve une uniformité considérable dans la distribution du coefficient de la transmission de chaleur sur la périphérie du tube. La différence des temperatures entre les points supérieurs et inférieurs de la section transversale du tube, fait en l'acier inoxydable, était égale à 9 K. On remarque que la température maximale de paroi sur la périphérie déplace relativement du point supérieur du tube. Les mesures locales de la température dans la section transversale de flux ont montré la présence de l'écoulement tourbillonnaire au canal. Le système tuorbillonnaire obtenu dans le flux explique le déplacement du point de la température maximale de la paroi de tube relativement du point supérieur. On propose la dépendance pour les coefficients locals et moyens de la transmission du chaleur dans le tube horizontale.

TABLE I

Experimental results; heat transfer to fluid helium flowing through a horizontal tube

a - REGIME N 2: p = 0.1216 MPa; Q = 28.7 W; G = 0.52 g/s; $\bar{T}_{b_1}$ = 15 K

x/L		0.146	0.26	0.375	0.57	0.759	0.814
$\bar{T}_b$ K		16.52	17.71	18.92	20.97	22.97	28.55
T_w	$\phi = 0$	24.2	25.35	26.25	28	31.7	25
	$\phi = \pi$	22.75	22.8	23.1	25	26.65	24.5
α W/m^2-K	$\phi = 0$	22	22.1	23	24	19.34	113.3
	$\phi = \pi$	27.1	33.2	40.38	41.9	45.86	177.7
Re · 10^{-4}		1.16	1.11	1.06	0.935	0.337	0.923
Pr		0.703	0.704	0.704	0.705	0.707	0.708
$Gr_q \cdot 10^{-9}$		0.573	0.404	0.291	0.174	0.111	0.0988
Nu	$\phi = 0$	16.586	16.003	16.036	15.68	11.381	71.15
	$\phi = \pi$	20.448	24.024	28.127	27.391	28.422	108
$\frac{Nu}{Nu_b}$	$\phi = 0$	0.465	0.465	0.482	0.496	0.398	2.33
	$\phi = \pi$	0.573	0.702	0.846	0.867	0.944	3.65
$\overline{Nu}_r$		0.516	0.578	0.631	0.655	0.613	2.9
ψ_ϕ	$\phi = 0$	1.46	1.44	1.40	1.34	1.39	1.07
	$\phi = \pi$	1.39	1.29	1.23	1.2	1.16	1.045
$\bar{\psi}_\phi$		1.431	1.36	1.3	1.231	1.25	1.045
Nu_π / Nu_0		1.23	1.509	1.755	1.748	2.37	1.56
$\frac{Gr_q}{Gr_L}$		180	143	116	83.25	67.2	58.1

TABLE I - Continued

b - REGIME N 6: p = 0.2047 MPa; Q = 67.7 W; G = 1.84 g/s; $\overline{T}_{b_1}$ = 10.35 K

x/L		0.146	0.260	0.375	0.57	0.759	0.814
$\overline{T}_b$K		11.31	12.07	12.85	14.17	15.46	15.857
T_w,K	$\phi = 0$	17.8	19	19.25	21.9	22	19
	$\phi = \pi$	15.7	15.4	16.25	17.3	17.25	17.5
α W/m^2-K	$\phi = 0$	61.37	57.48	62.24	51.5	60.93	126
	$\phi = \pi$	90.74	119.66	117.2	127.23	222	254
$Re \cdot 10^{-4}$		5.158	4.948	4.75	4.469	4.225	4.16
Pr		0.727	0.723	0.72	0.716	0.714	0.713
$Gr_q \cdot 10^{-10}$		2.69	1.9	1.36	0.813	0.523	0.461
Nu	$\phi = 0$	57.238	51.477	53.608	41.961	47.273	96.03
	$\phi = \pi$	84.624	107.161	100.936	103.629	173.001	182.647
$\frac{Nu}{Nu_b}$	$\phi = 0$	0.481	0.447	0.482	0.397	0.47	0.96
	$\phi = \pi$	0.71	0.93	0.907	0.98	1.73	1.83
$\overline{Nu}_r$		0.584	0.644	0.661	0.624	0.901	1.32
ψ_ϕ	$\phi = 0$	1.65	1.63	1.54	1.58	1.44	1.2
	$\phi = \pi$	1.44	1.29	1.29	1.23	1.11	1.1
$\overline{\psi}_\phi$		1.533	1.442	1.397	1.373	1.23	1.153
Nu_π/Nu_0		1.478	2.082	1.883	2.47	3.66	1.902
$\frac{Gr_q}{Gr_L}$		131	104	83.95	60	45.1	41.5

TABLE I - Continued

c - REGIME N 10: p = 0.304 MPa; Q = 210 W; G = 4.7 g/s; $\overline{T}_{b_1}$ = 7.0 K

x/L		0.146	0.260	0.375	0.57	0.753	0.814
$\overline{T}_b$K		7.9	8.679	9.516	10.999	12.496	12.93
T_w,K	$\phi = 0$	18.6	19.4	20	23.4	26.75	21.35
	$\phi = \pi$	16.25	15.45	15.9	16.9	17.8	16.3
α W/m^2-K	$\phi = 0$	19.626	19.58	20.03	16.93	14.73	24.9
	$\phi = \pi$	25.15	31	32.89	35.6	39.59	62.3
$Re \cdot 10^{-5}$		1.56	1.48	1.407	1.298	1.21	1.18
Pr		0.887	0.831	0.795	0.761	0.745	0.741
$Gr_q \cdot 10^{-12}$		1.76	0.925	0.517	0.222	0.112	0.0928
Nu	$\phi = 0$	127.483	121.287	118.485	91.950	74.638	123.98
	$\phi = \pi$	163.369	192.047	194.58	193.235	200.6	309.76
$\frac{Nu}{Nu_b}$	$\phi = 0$	0.41	0.414	0.428	0.362	0.314	0.531
	$\phi = \pi$	0.525	0.656	0.705	0.76	0.844	1.38
$\overline{Nu}_r$		0.464	0.521	0.549	0.524	0.514	0.84
ψ_ϕ	$\phi = 0$	3.18	2.79	2.61	2.38	2.32	1.74
	$\phi = \pi$	2.7	2.13	2.0	1.66	1.49	1.3
$\overline{\psi}_\phi$		2.94	2.414	2.137	1.941	1.805	1.47
Nu_π/Nu_0		1.28	1.583	1.642	2.1	2.68	2.45
$\frac{Gr_q}{Gr_L}$		343	217	145	81.3	50.91	44.8

TABLE I - Continued

d - REGIME N 14: p = 0.1824 MPa; Q = 65.3 W; G = 1.08 g/s; $\overline{T}_{b_1}$ = 6.5 K

x/L -		0.146	0.260	0.375	0.57	0.759	0.814
$\overline{T}_b$K		7.909	9.092	10.336	12.481	14.6	15.212
T_w,K	$\phi = 0$	21.4	22.6	22.11	22.2	22.8	21.5
	$\phi = \pi$	20.1	20.4	19.4	18.4	17.5	14.3
α W/m²-K	$\phi = 0$	91.5	91.4	105	127	150.6	------
	$\phi = \pi$	101.3	109.2	136.2	208.7	425.9	------
$Re \cdot 10^{-4}$		3.81	3.5	3.22	2.85	2.58	2.51
Pr		0.772	0.774	0.728	0.717	0.712	0.711
$Gr_q \cdot 10^{-10}$		16	6.99	3.43	1.24	0.549	0.443
Nu	$\phi = 0$	33.065	30.468	32.293	34.873	37.642	47.808
	$\phi = \pi$	36.591	36.395	41.913	57.261	106.437	------
$\frac{Nu}{Nu_b}$	$\phi = 0$	0.345	0.345	0.394	0.472	0.553	------
	$\phi = \pi$	0.381	0.413	0.512	0.776	1.56	------
$\overline{Nu_r}$		0.362	0.377	0.449	0.605	0.928	------
ψ_ϕ	$\phi = 0$	4.18	3.38	2.92	2.43	2.16	2.09
	$\phi = \pi$	3.9	3.02	2.53	1.99	1.62	1.26
$\overline{\psi}_\phi$		4	3.12	2.64	2.1	1.8	------
Nu_π/Nu_0		1.107	1.195	1.298	1.642	2.828	------
$\frac{Gr_q}{Gr_L}$		1600	976	612	313	185	------

TABLE I - Concluded

e - REGIME N 15: p = 0.2533 MPa; Q = 66.3 W; G = 1.08 g/s; $\overline{T}_{b_1}$ = 6.8 K

x/L -		0.146	0.260	0.375	0.57	0.759	0.814
$\overline{T}_b$K		8.119	9.273	10.499	12.633	14.754	15.367
T_w,K	$\phi = 0$	25.4	23.6	22.5	22.5	23.1	22.2
	$\phi = \pi$	22.3	21.4	19.7	18.8	18.7	16.7
α W/m²-K	$\phi = 0$	22.57	27.22	32.5	39.13	46.17	61.9
	$\phi = \pi$	27.1	32.42	41.935	62.2	97.5	487
$Re \cdot 10^{-4}$		3.62	3.35	3.118	2.785	2.531	2.469
Pr		0.822	0.776	0.752	0.732	0.723	0.721
$Gr_q \cdot 10^{-10}$		29.6	12.8	6.37	2.21	1.01	0.825
Nu	$\phi = 0$	25.231	28.16	31.281	33.862	36.455	-------
	$\phi = \pi$	30.32	33.545	30.361	53.854	76.9	-------
$\frac{Nu}{Nu_b}$	$\phi = 0$	0.268	0.325	0.387	0.463	0.542	5.27
	$\phi = \pi$	0.321	0.3187	0.5[illegible]	0.737	1.14	0.669
$\overline{Nu_r}$		0.293	0.355	0.44	0.584	0.786	1.87
ψ_ϕ	$\phi = 0$	3.99	3.43	2.35	1.87	1.62	-------
	$\phi = \pi$	3.45	2.67	2.03	1.54	1.3	-------
$\overline{\psi}_\phi$		3.77	2.81	2.21	1.7	1.0735	-------
Nu_π/Nu_0		1.202	1.191	1.29	1.59	2.109	-------
$\frac{Gr_q}{Gr_L}$		3421	1933	1211	616	353	-------

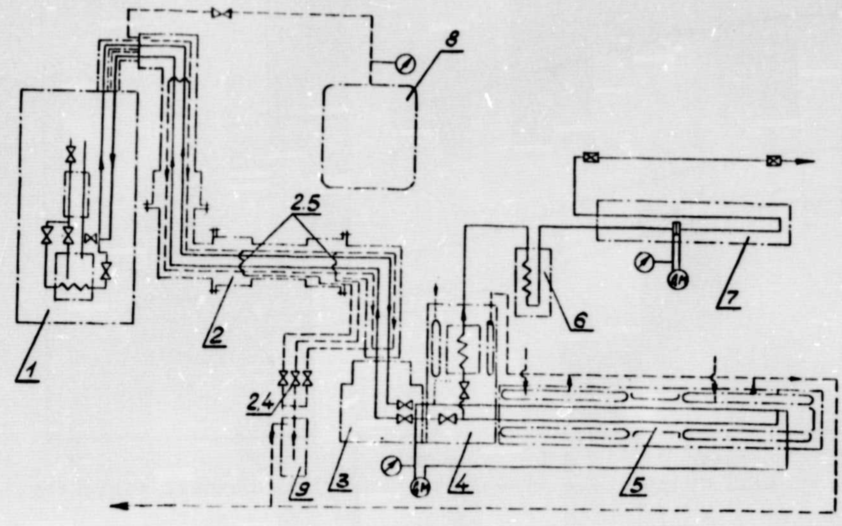

Fig. 1 Experimental flow loop.

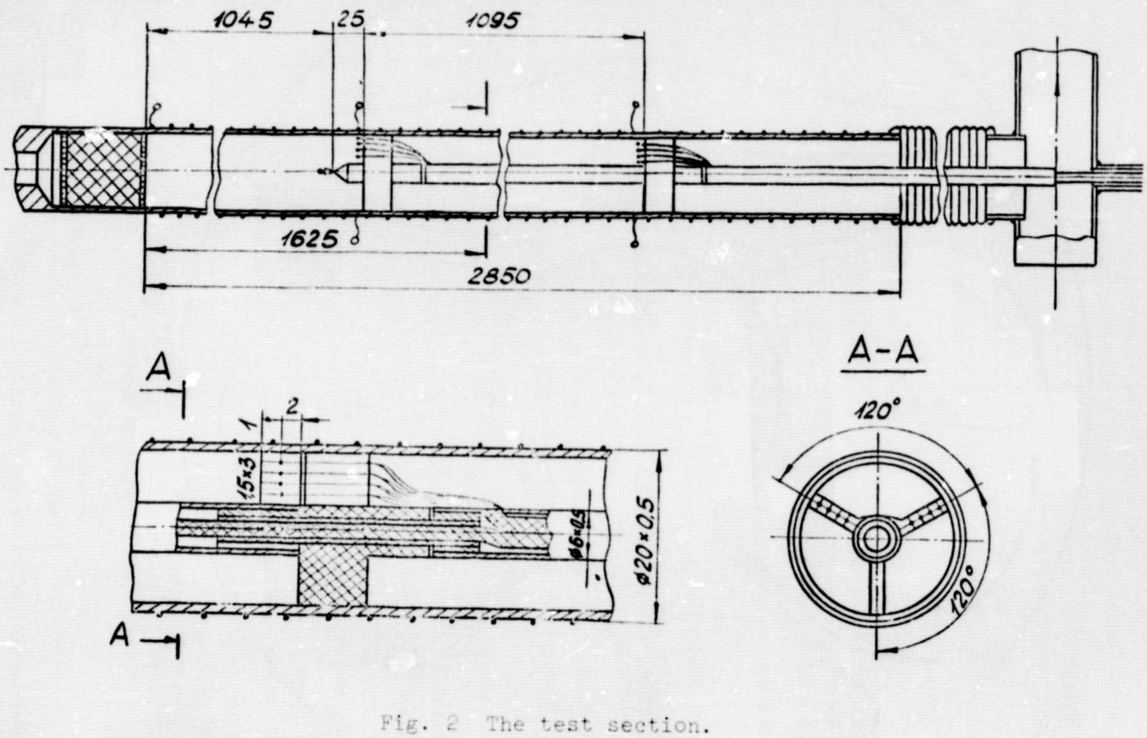

Fig. 2 The test section.

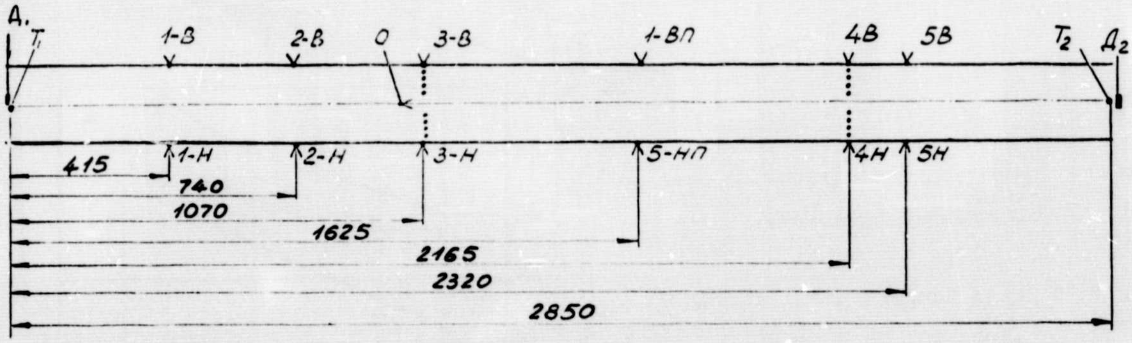

Fig. 3 Positions of thermometers and thermocouples along the test section.

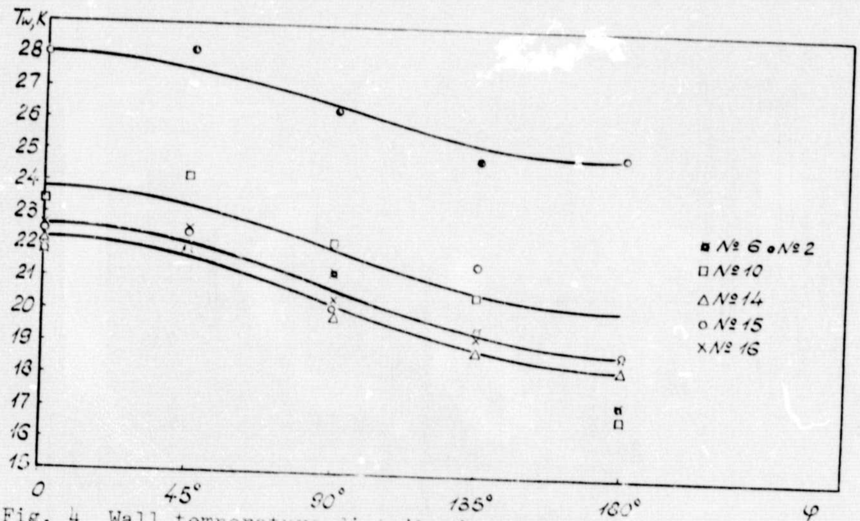

Fig. 4 Wall temperature distribution over the channel periphery.

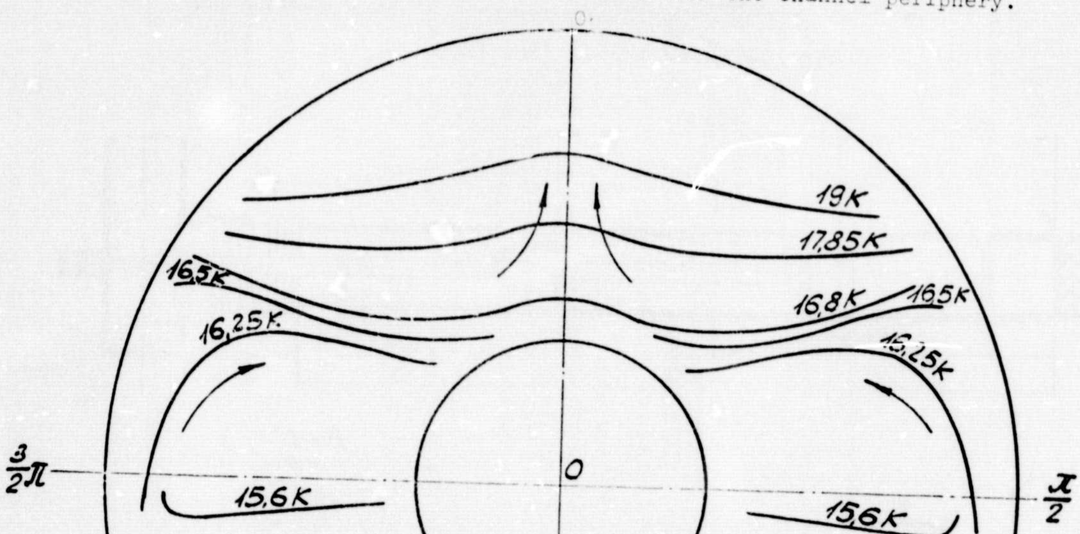

Fig. 5 Temperature distribution over the channel periphery.

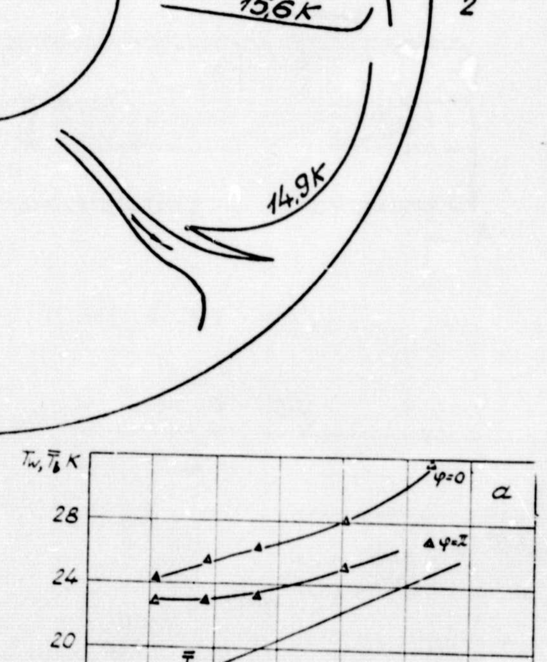

Fig. 6 Wall temperature distribution along the test section:
a - regime 2.

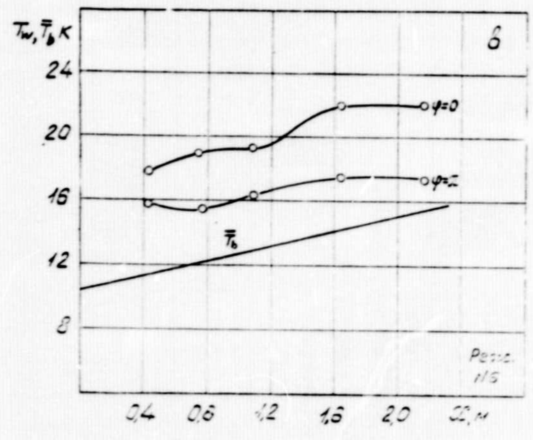

Fig. 6 Continued.
b - regime 6.

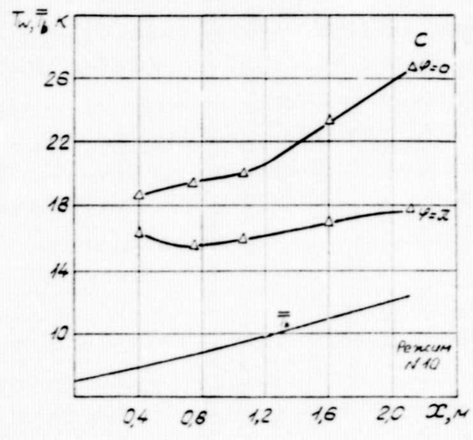

Fig. 6 Continued.
c - regime 10.

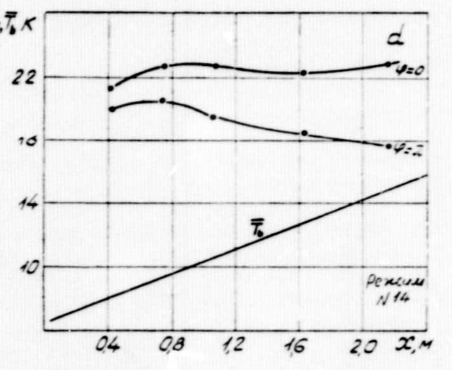

Fig. 6 Continued.
d - regime 14.

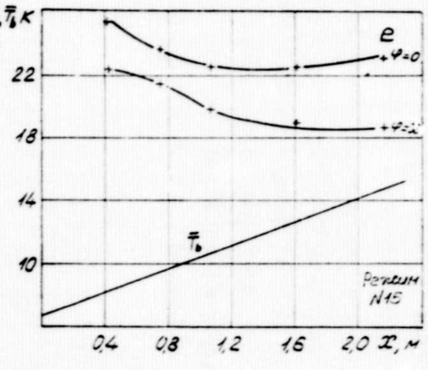

Fig. 6 Concluded.
e - regime 15.

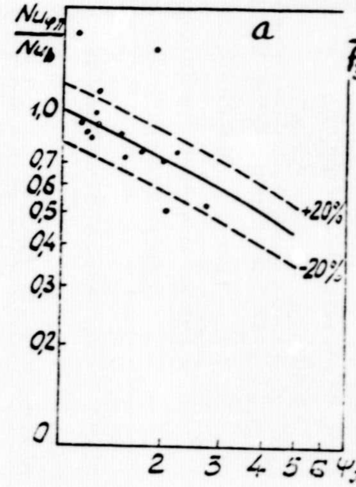

a - lower surface.

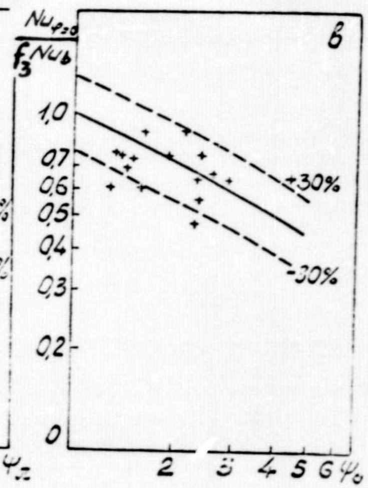

b - upper surface.

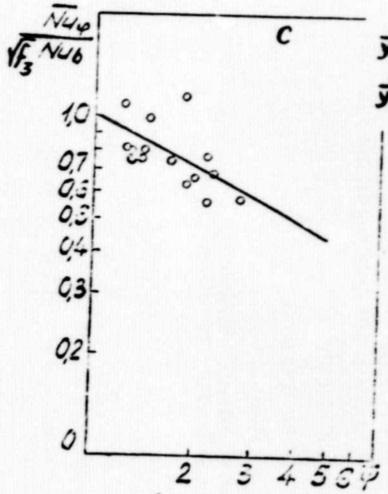

c - value averaged over the wall periphery.

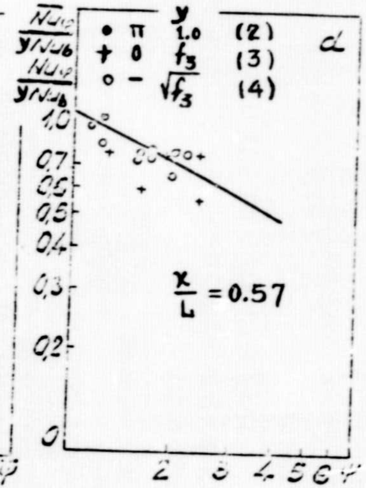

d - local heat transfer over periphery at x/L = 0.57.

Fig. 7 Correlation of experimental data obtained;